LRP 355/88 September 1988

TOKAMAK EQUILIBRIUM RECONSTRUCTION USING FARADAY ROTATION IN MEASUREMENTS

F. Hofmann and G. Tonetti

to be published in Nuclear Fusion

TOKAMAK EQUILIBRIUM RECONSTRUCTION USING FARADAY ROTATION MEASUREMENTS

F. Hofmann and G. Tonetti

Centre de Recherches en Physique des Plasmas
Association Euratom - Confédération Suisse
Ecole Polytechnique Fédérale de Lausanne
21, Av. des Bains, CH - 1007 Lausanne, Switzerland

ABSTRACT

A new equilibrium reconstruction procedure using magnetic, line-integrated electron density and Faraday rotation measurements has been developed. The method has been applied to a number of elongated tokamak equilibria which were computed by using a free-boundary MHD equilibrium code. Typical errors in four global plasma parameters (β_p, l_i, μ and q_0) are evaluated as functions of the measurement errors and the number of source function parameters. Assuming realistic random perturbations in the measurements, the method allows the reconstruction of source functions with up to six independent parameters. It is shown that, when electron density and Faraday rotation measurements are included, the accuracy in the determination of q_0 is increased by at least a factor 2, as compared to cases without Faraday rotation data. The effects of adding a diamagnetic probe and of varying the plasma elongation are also investigated.

1. INTRODUCTION

The problem of reconstructing tokamak equilibria, based on external measurements, is becoming increasingly important in view of the recent evolution towards highly elongated and shaped plasmas. The problem consists of finding a solution to the Grad-Shafranov equation, with arbitrary source functions, such that the measurements are reproduced as well as possible. Two circumstances complicate the solution of this problem: (a) it is mathematically ill-posed and (b) all measurements are subject to errors. Consequently, there is no rigorously accurate and no unique solution.

Equilibrium reconstruction methods can be divided in two groups, i.e. those which do and those which do not solve the Grad-Shafranov equation. We only consider the first group here. The methods in this group [1 - 8] differ from one another in the numerical algorithms and the type of measurements which are used. All methods use magnetic measurements (ψ and B) close to the vessel wall and, in addition, some methods use pressure profiles [3], diamagnetic signals [7], soft x-ray measurements [6] or the value of the safety factor on axis, q_o [1], for reconstructing the equilibrium. In several of these studies it has been shown that the use of additional measurements (other than ψ and B) allows a more accurate solution to be found, in the sense that the number of source function parameters that can be reliably determined is increased.

In this paper we propose to use line-integrated electron density and Faraday rotation measurements [9] together with the standard magnetic measurements, to improve the accuracy of equilibrium reconstructions.

2. EQUILIBRIUM RECONSTRUCTION USING FARADAY ROTATION MEASUREMENTS

When one tries to reconstruct tokamak equilibria with arbitrary source functions, using magnetic measurements, one soon encounters a fundamental problem: The toroidal plasma current density must be split into two parts, one being proportional to Rp' and the other to TT'/R, where R is the major radius, p is the plasma pressure, $T = RB_{tor}$ and the prime denotes differentiation with respect to ψ. The relative importance of these two terms can, in principle, be determined thanks to the difference in their R-dependence. The accuracy of the decomposition, however, depends on the radial extent of the flux surface under consideration. For the outer flux surfaces, the decomposition can be performed quite accurately but as one approaches the magnetic axis, the accuracy decreases rapidly. On axis, where the radial extent of the flux surface shrinks to zero, it becomes impossible to compute p' and TT' separately. In fact, the values of p' and TT' on axis are generally obtained by extrapolation from the outer regions. The validity of this extrapolation depends essentially on the size of the measurement errors and on the type of measurements being used. Faraday rotation measurements can provide additional information on the poloidal magnetic field inside the plasma. We expect, therefore, that the accuracy of an equilibrium reconstruction should be considerably improved by using such measurements.

Let us assume that, in the reconstructed equilibrium, source functions and electron density can be expressed in terms of the poloidal flux,

$$p' = \sum_{n=0}^{N_p} a_n U_n(\phi) \qquad (1)$$

$$TT' = \sum_{n=0}^{N_T} b_n V_n(\phi) \tag{2}$$

$$n_e = \sum_{n=0}^{N_n} c_n W_n(\phi) \tag{3}$$

where a_n, b_n, c_n, are constants to be determined, $U_n(\phi)$, $V_n(\phi)$, $W_n(\phi)$ are arbitrary basis functions and $\phi = (\psi - \psi_{lim})/(\psi_{ax} - \psi_{lim})$. ψ_{lim} and ψ_{ax} are the values of the poloidal flux function at the limiter and on the magnetic axis, respectively. It should be noted that eq. (3) is not always a good approximation. In cases with high toroidal rotation velocity, for example, the radial density profile is shifted with respect to the ψ-profile and n_e is no longer a single-valued function of ψ. These cases are not considered here.

The basis functions, U_n, V_n, and W_n, can be specified arbitrarily. For the purpose of this study we assume

$$\left.\begin{aligned}
U_0 &= V_0 = (1-\phi)^2 \\
U_1 &= V_1 = \phi \\
U_2 &= V_2 = 1-(2\phi-1)^2 \\
U_3 &= V_3 = (2\phi-1)\left[1-(2\phi-1)^2\right] \\
W_n &= \phi^n
\end{aligned}\right\} \tag{4}$$

The equilibrium reconstruction problem, being intrinsically non-linear, is solved by an iterative procedure [1-8]. The method which has been used in the present study consists of the following steps:

(A) A rough approximation to the plasma current distribution is found by using one of the fast, magnetostatic methods, e.g. [10].

(B) The Grad-Shafranov equation is solved, using the measured flux values as the boundary condition. The flux surface defining the plasma boundary is then determined by searching for the limiter or X-point with the highest flux value.

(C) The profile parameters (a_n, b_n, c_n) are computed such as to obtain the best fit to the measurements, assuming $\Psi(R,Z)$ fixed.

(D) The toroidal plasma current density, $j = Rp^{\prime} + (R\mu_o)^{-1}TT^{\prime}$, is computed using the expressions (1) and (2).

(E) Steps B, C and D are repeated until a suitable convergence criterion is satisfied.

This procedure is fairly straightforward except for step C which is described below. We assume that the line-integrated electron density and the Faraday rotation angle are measured along a number of vertical chords,

$$N_i = \int_{L_i} n_e \, dZ \tag{5}$$

$$F_j = \int_{L_j} n_e B_Z \, dZ \tag{6}$$

It should be noted that the two sets of chords, L_i and L_j, may, but do not have to coincide. Using eq. (3), the reconstructed line densities, N_i^*, are written as

$$N_i^* = \int_{L_i} \sum_{n=0}^{N_n} c_n W_n(\phi)\, dZ = \sum_{n=0}^{N_n} G_{i,n}\, c_n \qquad (7)$$

where $G_{i,n}$ is a known matrix depending on $\Psi(R,Z)$. Optimum values of the density profile parameters, c_n, are found by minimizing the quantity

$$S_1 = \sum_i \left(\frac{N_i - N_i^*}{\Delta N_i} \right)^2 \qquad (8)$$

using the singular value decomposition method [11]. ΔN_i is the typical RMS error associated with the measurement N_i.

The source function parameters, a_n and b_n, can now be computed analogously since, with fixed values c_n, the nonlinearity of eq. (6) has been eliminated. Let the measurements of flux, magnetic field, Faraday rotation angle, plasma current and diamagnetic flux be given by the vectors and scalars $\vec{\psi}$, $\vec{B}$, $\vec{F}$, I_p and μ, respectively. The corresponding reconstructed (starred) quantities can be written

$$\left.\begin{aligned}
\vec{\Psi}^* &= A_1 \vec{I_c} + A_2 \vec{X} \\
\vec{B}^* &= A_3 \vec{I_c} + A_4 \vec{X} \\
\vec{F}^* &= E_1 \vec{I_c} + E_2 \vec{X} \\
I_p^* &= \vec{Q}_1 \cdot \vec{X} \\
\mu^* &= \vec{Q}_2 \cdot \vec{X}
\end{aligned}\right\} \qquad (9)$$

where $\vec{I_c}$ contains the measured currents in poloidal field coils and vacuum vessel, $\vec{X}$ is composed of the elements a_n, b_n and the matrices A_1, A_2, A_3, A_4, E_1 and E_2 contain Green's functions and their spatial derivatives. The matrices A_2, A_4, E_1 and E_2, as well as the vectors $\vec{Q_1}$ and $\vec{Q_2}$, depend on ψ

(R, Z). They therefore have to be recomputed at every iteration. In addition, the matrices E_1 and E_2 are functions of the density profile parameters, c_n.

We now combine all measurements (except N_i) into a single vector $\vec{M}$ and the corresponding reconstructed quantities into $\vec{M}^*$. The elements of the vector $\vec{X}$ are then determined by minimizing the function

$$S_2 = \sum_i \left(\frac{M_i - M_i^*}{\Delta M_i} \right)^2 , \tag{10}$$

where ΔM_i is the RMS error associated with the measurement M_i, again using the singular value decomposition procedure [11]. It should be noted that, in computing the measurement errors ΔM_i, the errors in $\vec{I}_c$ must also be taken into account.

3. EFFECT OF MEASUREMENT ERRORS

In order to evaluate the effect of measurement errors on the parameters of the reconstructed equilibrium, let us first consider a specific example, i.e. the reconstruction of a D-shaped equilibrium as shown in Fig. 1. The equilibrium was computed [12] in such a way that the pressure and q-profiles closely agree with experimental profiles, measured in the JET tokamak (pulse 10363) [13]. This was achieved by using the source functions,

$$\left.\begin{aligned} p' &= c_p\left[1.2 + 0.85(1-\phi)^{2.5} - 1.85(1-\phi)^{3.5}\right] \\ TT' &= c_T \mu_0 R_0^2\left[1 - 0.8(1-\phi) - 1.75(1-\phi)^4 + 1.5(1-\phi)^5\right] \end{aligned}\right\} \tag{11}$$

with $c_p/c_T=0.25$. The electron density profile, $n_e(\phi)$, was also obtained from the JET measurements [13].

In reconstructing this equilibrium, we proceed in exactly the same way as if we were dealing with experimental data: The only information available to the reconstruction algorithm is a number of simulated measurements, obtained from the output of the equilibrium code. We assume 44 flux loops, 44 magnetic field probes, oriented parallel to the wall, and 10 vertical chords for line-integrated electron density and Faraday-rotation measurements. The diamagnetic probe is not used in this example. Probe positions and chords are indicated in Fig. 1. Here, the line-density chords coincide with the Faraday rotation chords, as is the case in most experiments [9]. It should be noted, however, that as far as the accuracy of the equilibrium reconstruction is concerned, it is completely irrelevant whether the two sets of chords coincide or not. The basis functions are assumed as specified in eq. (4), with $N_p=2$, $N_T=1$, $N_n=3$. We further impose the condition, $\mu_0 R_0{}^2 a_0+b_0=0$, which ensures that the current density, averaged over the plasma boundary ($\phi=0$), is close to zero.

Measurement errors are taken into account by adding random perturbations to the values obtained from the equilibrium code. For each type of measurement, the maximum amplitude of these random errors is assumed to be constant and equal to a certain percentage of the highest measured signal. In order to demonstrate the effect of these errors on the parameters of the reconstructed equilibrium, we consider two cases, with error levels of ±2% and ±4%, respectively. For each case, we compute ten reconstructions with different initialization of the random number generator.

The results are summarized in Table 1. By computing the error of the mean value as well as the RMS error, we can distinguish between systematic errors, due to the truncation of the polynomial expansions (eqns. (1) - (4)), and pure random errors caused by the perturbation of the measurements. If there were no systematic errors, the error of the mean value should be of the order of one third of the RMS error. If, on the other hand, the error of the mean value is much larger than the RMS error, a systematic error must be involved. We note from Table 1. that systematic errors are generally insignificant, indicating that the number of source function parameters was sufficiently large in this particular case. The choice of optimum values of N_p and N_T will be discussed in the next section. We also note that the largest relative RMS errors appear in p_{max}, β_p and β_T. This is partly due to the small absolute value of β_p. It should be pointed out, on the other hand, that the maximum total error in q_o is only 5% in the case with ±2% random errors. In Fig. 2. we compare the source functions and density profiles of the original equilibrium with those obtained from one of the reconstructions discussed above.

4. OPTIMUM NUMBER OF SOURCE FUNCTION PARAMETERS

The error analysis presented in the previous section allows us to get an estimate of the optimum number of source function parameters to be used in a particular application. Figure 3 shows the results of 270 reconstructions of a D-shaped equilibrium, similar to the one shown in Fig.1. Errors in four global plasma parameters (β_p,ℓ_i,μ,q_o) are analyzed as a function of the numbers of source function parameters, with and without Faraday rotation measurements. Each data point in Fig. 3 is obtained from a statistical analysis of ten reconstruction calculations. Errors are shown in absolute value.

We note that, in general, the error of the mean value decreases and the RMS error increases with increasing numbers of source function parameters. Optimum values of N_p and N_T are found by searching for the minimum total error. Without Faraday rotation measurements (Case A), values of $N_p>2$ or $N_T>2$ must be avoided because this leads to a very large uncertainty in q_0. The addition of line-integrated electron density and Faraday rotation data (Cases B and C) allows the determination of up to six independent source function parameters. Figure 4 shows original and reconstructed source functions corresponding to Case C of Fig. 3, with $N_p=3$, $N_T=3$.

The method for finding optimum values of N_p and N_T, as outlined above, is not restricted to the analysis of computed equilibria. It can also be used in the case of a reconstruction based on experimental measurements, if the accuracy of these measurements is known. In this case one would look for convergence of the mean values as the number of parameters is increased, and one would chose those values of N_p and N_T which give the converged mean values with minimum RMS error.

5. DETERMINATION OF q_0

It is well known [1] that, using equilibrium reconstruction procedures based on magnetic measurements alone, it is very difficult to reproduce the value of the safety factor on axis (q_0) with good accuracy. In order to demonstrate the gain in accuracy due to the inclusion of line-integrated electron density and Faraday rotation measurements, we have done a large number of reconstruction calculations, with and without Faraday rotation data. Table 2 shows typical errors in q_0 for a variety of equilibria, covering wide ranges in parameter space. The total error is defined here as the sum of the error of the mean value of ten reconstructions and the RMS error. It is seen that the error in q_0 is reduced considerably, i.e. by factors between 2 and 4, by using the Faraday rotation measurements.

6. DIAMAGNETIC PROBE

It has been pointed out [7] that the use of a diamagnetic signal can considerably improve the accuracy of equilibrium reconstructions. In the procedure presented here, the diamagnetic probe is available as an option, and the question arises how accurate this probe should be in order to have a significant effect on the reconstruction. Figure 3, Case A, shows that the typical error in the plasma diamagnetism, without using a diamagnetic probe and without Faraday rotation measurements, is ~ 5 %. We therefore expect that under these circumstances, a diamagnetic probe would have to have an accuracy of the order of 5% if it is to make a significant contribution. This conjecture is verified in Fig. 5, where we show equilibrium reconstructions with and without diamagnetic probe. Case A of Fig. 5 is identical with Case A of Fig. 3, assuming $N_p = 2$, $N_T = 1$. Cases B and C of Fig. 5 include the diamagnetic probe with ± 4% and ± 2% error levels, respectively. It is seen that the use of the diamagnetic signal reduces the RMS error on the plasma diamagnetism considerably, as expected. It also reduces the RMS error on β_p. The parameters ℓ_i and q_0, however, are practically unaffected. It should be noted that, from an experimental point of view, it is extremely difficult to obtain a diamagnetic signal with 4% accuracy, and 2% accuracy is probably beyond the current state of the art [14].

7. EFFECT OF ELONGATION

Up to this point, we have been considering exclusively D-shaped equilibria with elongation K=2.0. In this section, we are interested in the question whether the elongation of the original equilibrium has an influence on the precision of the reconstructed parameters. For this purpose, we consider three cases with elongations between 2.0 and 3.0 (Fig. 6). Probe positions and chords for line-integrated electron density and Faraday rotation measurements are the same as in Fig. 1. Random errors of ± 2% of the maximum signal were assumed on all measurements. Typical errors in the four reconstructed plasma parameters are shown in Fig. 7. As usual, each data point is the result of ten reconstruction calculations. We note that, in the range of plasma elongations considered here, the elongation does not significantly affect the precision of the reconstruction. It is known, on the other hand, that for near-circular plasmas ($1.0 < K < 1.5$), the elongation can have a decisive influence on the accuracy of the reconstructed β_p and ℓ_i values [5].

8. CONCLUSION

The equilibrium reconstruction procedure presented in this paper, using Faraday rotation, electron density and magnetic measurements, allows the determination of source functions with up to six free parameters. The optimum number of source function parameters to be used in a particular application depends on the precision and type of measurements available and on the properties of the equilibrium being analyzed. Typically, the best compromise between systematic and random errors is obtained with three to five independent parameters. The analysis of a number of equilibria with widely varying parameters has shown that the error in q_0 can be reduced by factors between 2 and 4 by using electron density and Faraday rotation measurements. Using a diamagnetic probe can improve the precision in the determination of μ and β_p, if the diamagnetic signal is sufficiently accurate. In a case with ±2% errors in the magnetic measurements, without using Faraday rotation data, the RMS error in the diamagnetic signal should be less than ~±4% if the probe is to be useful. Finally, we show that the method is applicable equally well to plasmas with elongation up to 3.0.

ACKNOWLEDGEMENTS

Fruitful discussions with Drs. R. Behn, L.L. Lao and F.B. Marcus are gratefully acknowledged. This work was partly supported by the Swiss National Science Foundation.

REFERENCES

[1] Lao, L.L. St. John, H., Stambaugh, R.D., Kellman, A.G., Pfeiffer, W., Nucl. Fusion 25 (1985) 1611.

[2] Brusati, M., Christiansen, J.P., Cordey, J.G., Jarrett, K., Lazzaro, E., Ross, R.T., Comput. Phys. Rep. 1 (1984) 345.

[3] Blum, J., Gilbert, J.Ch., Thooris, B., Paramagnetic Identifiation of the Plasma Current Density from Magnetic Measurement and Pressure Profile, Rep. JET, Contract No. JT3/9008, JET Joint Undertaking, Abingdon, Oxfordshire (1985).

[4] Braams , B.J., in Controlled Fusion and Plasma Physics (Proc. 12th Europ. Conf. Budapest, 1985), Vol. 9F, Part I, European Physical Society (1985) 167.

[5] Lao, L.L., St. John, H. Stambaugh, R.D., Pfeiffer, W., Nucl. Fusion 25 (1985) 1421.

[6] Christiansen, J.P., Callen, J.D., Granetz, R., Bull. Amer. Phys. Soc. 32 (1987) 1768.

[7] Kuznetsov, Yu. K., Pyatov, V.N., Yasin, I.V., Sov. J. Plasma Phys. 13 (1987) 75.

[8] Luxon, J.L., Brown, B.B., Nucl. Fusion 22 (1982) 813.

[9] Soltwisch, H., Stodiek, W., Manickam, J., Schlüter, J., in Plasma Physics and Controlled Nuclear Fusion Research 1986 (Proc. 11th Int. Conf. Kyoto, 1986), Vol. 1, IAEA, Vienna (1987) 263; Soltwisch, H., Rev. Sci. Instrum. 57 (1986) 1939.

[10] Hofmann, F., Tonetti, G., Nucl. Fusion 28 (1988) 519.

[11] Forsythe, G.E., Malcolm, M.A., Moler, C.B., Computer Methods for Mathematical Computations, Prentice-Hall, Englewood Cliffs, N.J. 1977.

[12] Hofmann, F., Comput. Phys. Commun. 48 (1988) 207.

[13] JET TEAM, presented by P.H. Rebut, in Plasma Physics and Controlled Nuclear Fusion Research 1986 (Proc. 11th Int. Conf. Kyoto, 1986) Vol.1, IAEA, Vienna (1987) 31.

[14] Tonetti, G., Christiansen, J.P., and de Kock, L., Rev. Sci. Instrum. 57 (1986) 2087.

FIGURE CAPTIONS

Fig. 1 D-shaped equilibrium with flux surfaces (solid lines), plasma boundary (dotted line), flux loops (closed circles), magnetic field probes (open circles), chords for line-integrated electron density and Faraday rotation measurements (dashed lines) and external currents (crosses). Pressure, current and q-profiles, at the height of the magnetic axis, are also shown.

Fig. 2 Original (solid lines) and reconstructed (dashed lines) source functions and electron density vs. normalized flux ϕ. N_p=2, N_T=1, N_n=3. Random measurement errors ± 2% of maximum signal.

Fig. 3 Errors of mean values (open circles) and RMS errors (bars) of four global plasma parameters. Cases A,B and C have random measurement errors of ± 2%, ± 2% and ± 1% respectively. Case A without, Cases B and C with Faraday rotation measurements. Numbers of source function parameters are shown at the bottom; N_n=2, a_o=b_o=0. Source functions see Fig 4.

Fig. 4 Original (solid lines) and reconstructed (dashed lines) source functions vs. normalized flux, ϕ. N_p=3, N_T=3, N_n=2, a_o=b_o=0. Random measurement errors ± 1% of maximum signal.

Fig. 5 Errors of mean values (open circles) and RMS errors (bars) in four plasma parameters. Case A without, Cases B and C with diamagnetic probe. Faraday rotation measurements are not used. Measurement errors in ψ , B and I_p ± 2% of maximum signal. Diamagnetic probe error ± 4% and ± 2% in cases B and C, respectively. N_p=2, N_T=1. a_o=b_o=0.

Fig. 6 Equilibria with increasing elongation (K):

A: K=2.0, β_p=0.2576, ℓ_i=0.6905, μ=0.5351, q_o=1.05;

B: K=2.5, β_p=0.2257, ℓ_i=0.6024, μ=0.4663, q_o=1.05;

C: K=3.0, β_p=0.1997, ℓ_i=0.5326, μ=0.4119, q_o=1.05.

Fig.7 Errors of mean values (open circles) and RMS errors (bars) vs. plasma elongation (K). Measurement errors ± 2% of maximum signal, diamagnetic probe not used. N_p=2, N_T=1, N_n=2, a_o=b_o=0.

Table I

	Exact Value	Error of mean value of 10 reconstructions %		RMS error %	
		A	B	A	B
Plasma current I_p [MA]	5.00	-0.51	-0.98	0.70	1.39
Poloidal beta, β_p	0.3482	-0.55	-1.11	6.0	12.9
Toroidal beta, β_T	0.0171	-0.68	-0.96	6.8	13.0
Radius of magnetic axis, R_{ax} [m]	2.991	-0.02	0.02	0.08	0.16
Height of magnetic axix, Z_{ax} [m]	0.802	0.44*	0.92*	0.64*	1.26*
Flux on axis, Ψ_{ax} [Vs]	1.810	0.67	0.47	0.82	1.62
Max. current density, j_{max} [MAm^{-2}]	2.399	3.03	3.74	1.99	4.06
Max. pressure, p_{max} [MPa]	0.2924	-3.01	1.90	6.65	12.20
Internal inductance, ℓ_i	0.7394	-0.44	0.30	1.33	2.71
Plasma diamagnetism, μ	0.4610	0.89	1.67	4.09	8.16
Safety factor on axis, q_o	1.050	-3.19	-4.11	2.39	4.66

* Percentage of R_{ax}

Measurement errors: A: ±2%, B: ±4% of maximum signal.

Table 2

Equilibrium No.	β_T %	β_p	ℓ_i	μ	q_o	q_s	Total error in q_o, %	
							without Faraday	with Fararay
1	0.33	0.394	0.804	0.429	2.00	9.17	8.4	3.4
2	0.49	0.726	0.822	0.115	2.00	10.52	8.8	3.6
3	0.97	0.195	0.733	0.603	1.05	3.55	11.3	3.1
4	1.25	0.394	0.804	0.429	1.05	4.71	9.2	3.6
5	1.43	0.128	0.595	0.635	1.05	2.12	20.8	4.8
6	1.58	0.324	0.740	0.483	1.05	3.65	7.9	4.3
7	1.75	0.452	0.754	0.359	1.05	4.11	8.5	4.0
8	1.80	0.726	0.822	0.115	1.05	5.50	9.3	3.7
9	2.06	0.369	0.683	0.422	1.05	3.24	11.3	3.2
10	4.45	0.826	0.691	0.0	1.05	3.49	8.7	4.2
11	6.09	0.998	0.671	-0.164	1.05	3.30	7.3	4.3
12	8.27	1.260	0.641	-0.410	1.05	3.22	9.4	4.7

$N_p = 2$, $N_T = 2$, $N_h = 3$, Measurement errors ±2% of maximum signal

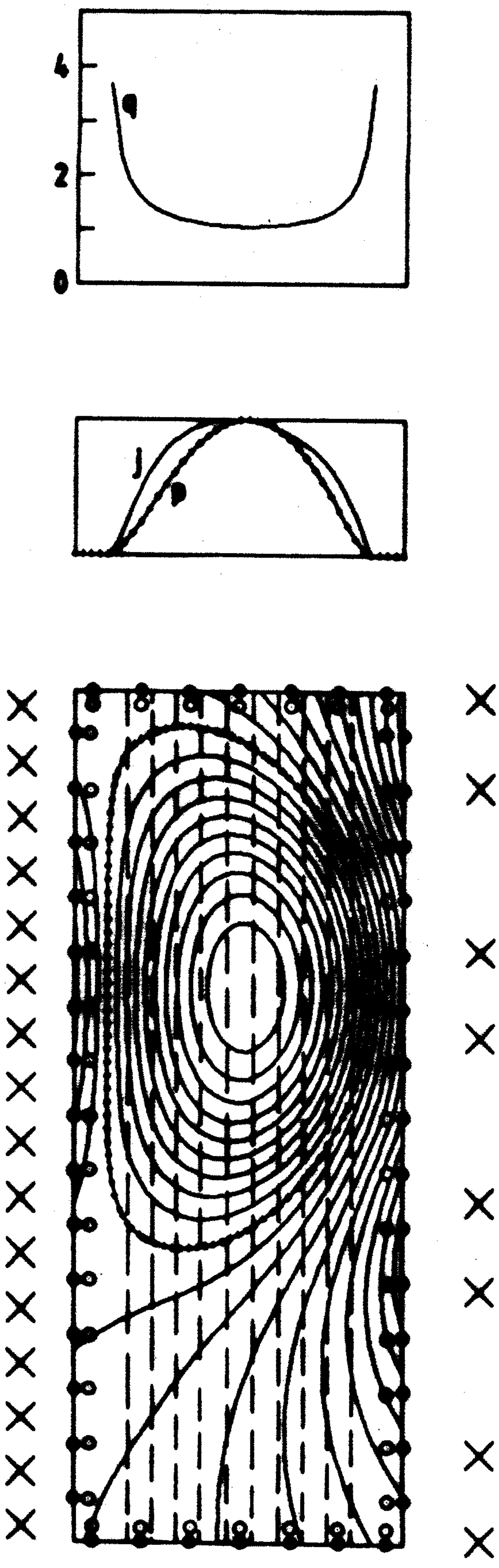

FIG. 1

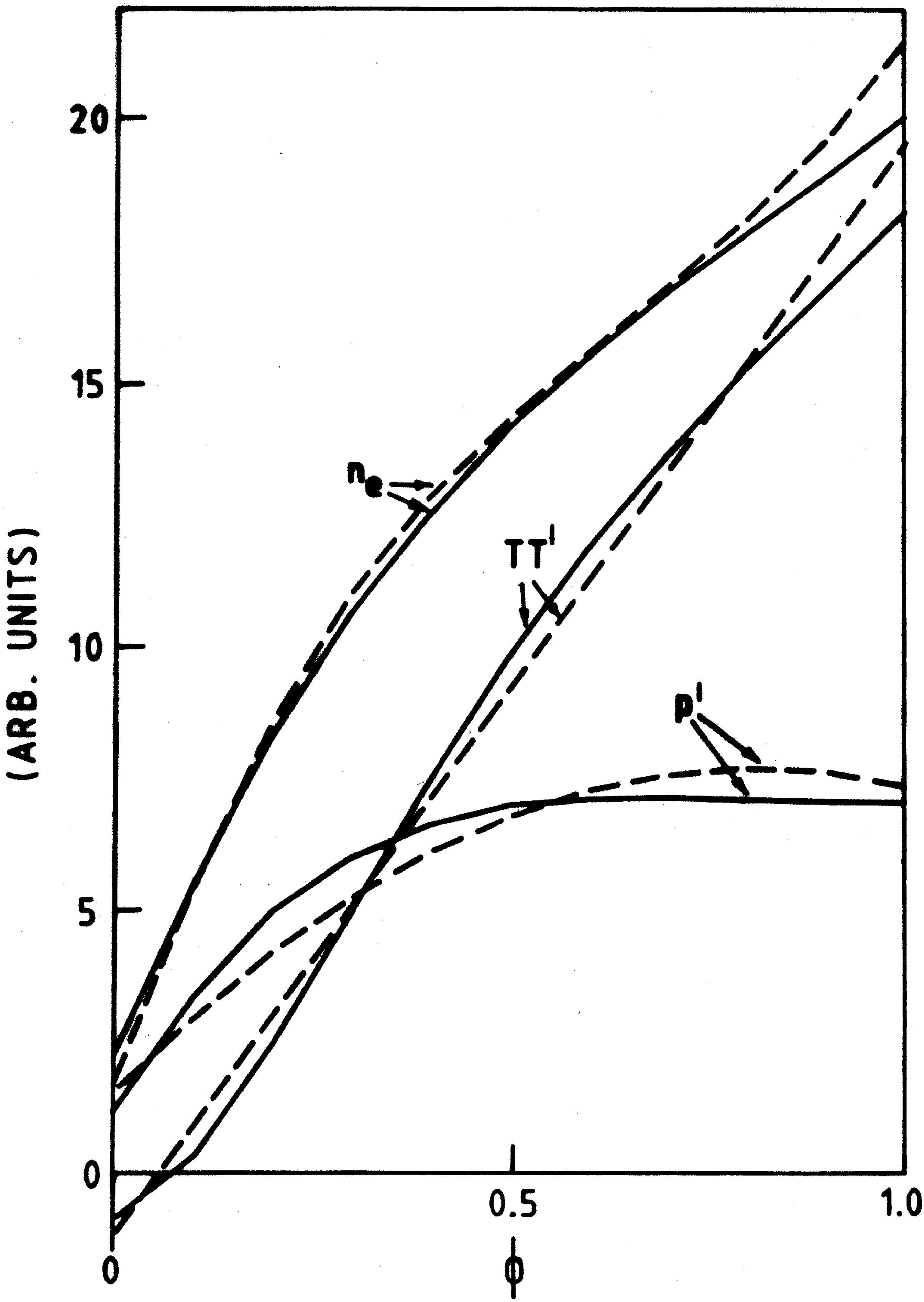

FIG.2

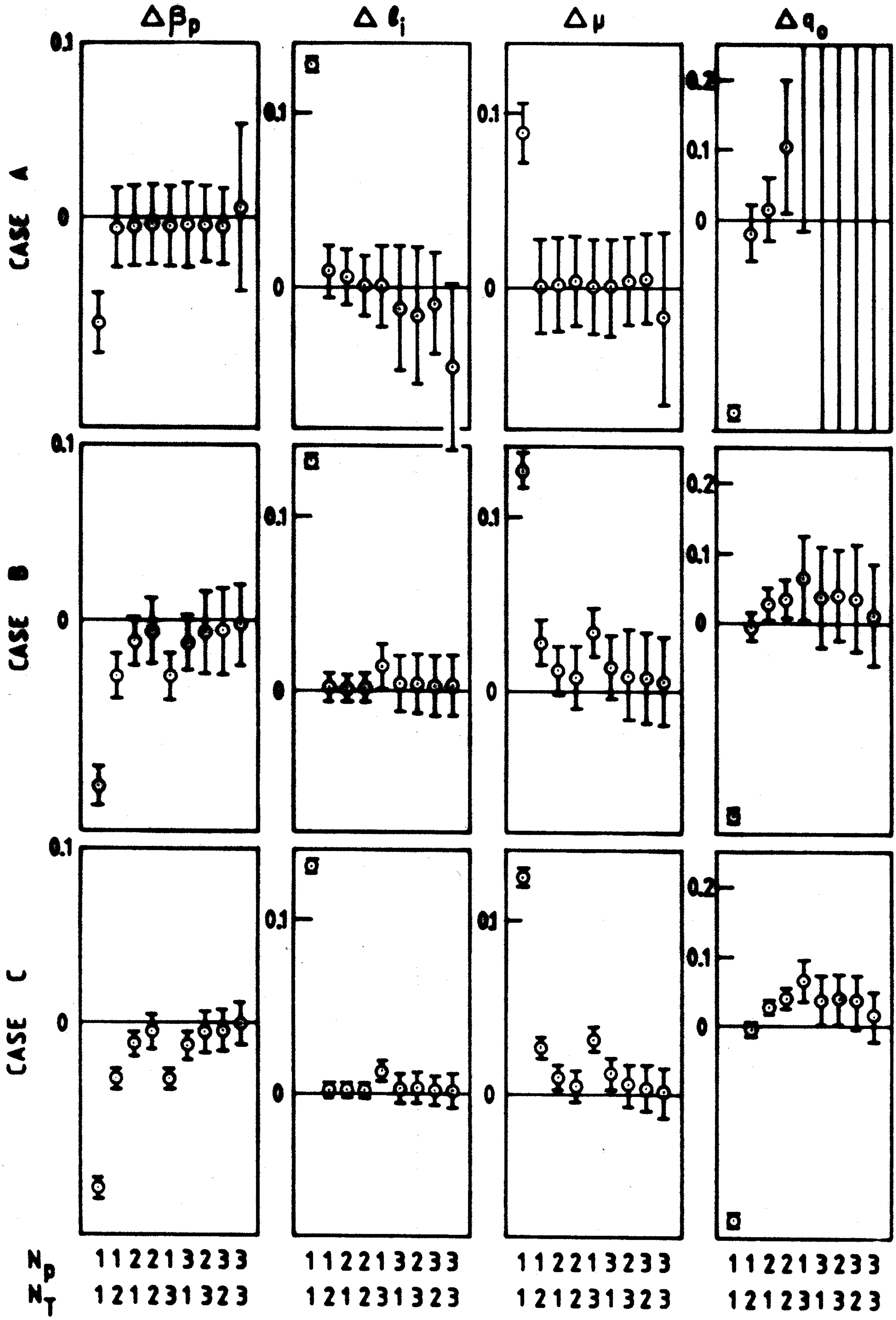

Δβp
Δℓi
Δμ
Δq0
CASE A
CASE B
CASE C
0.1
0
0.2
Np
NT
1 1 2 2 1 3 2 3 3
1 2 1 2 3 1 3 2 3

FIG.3

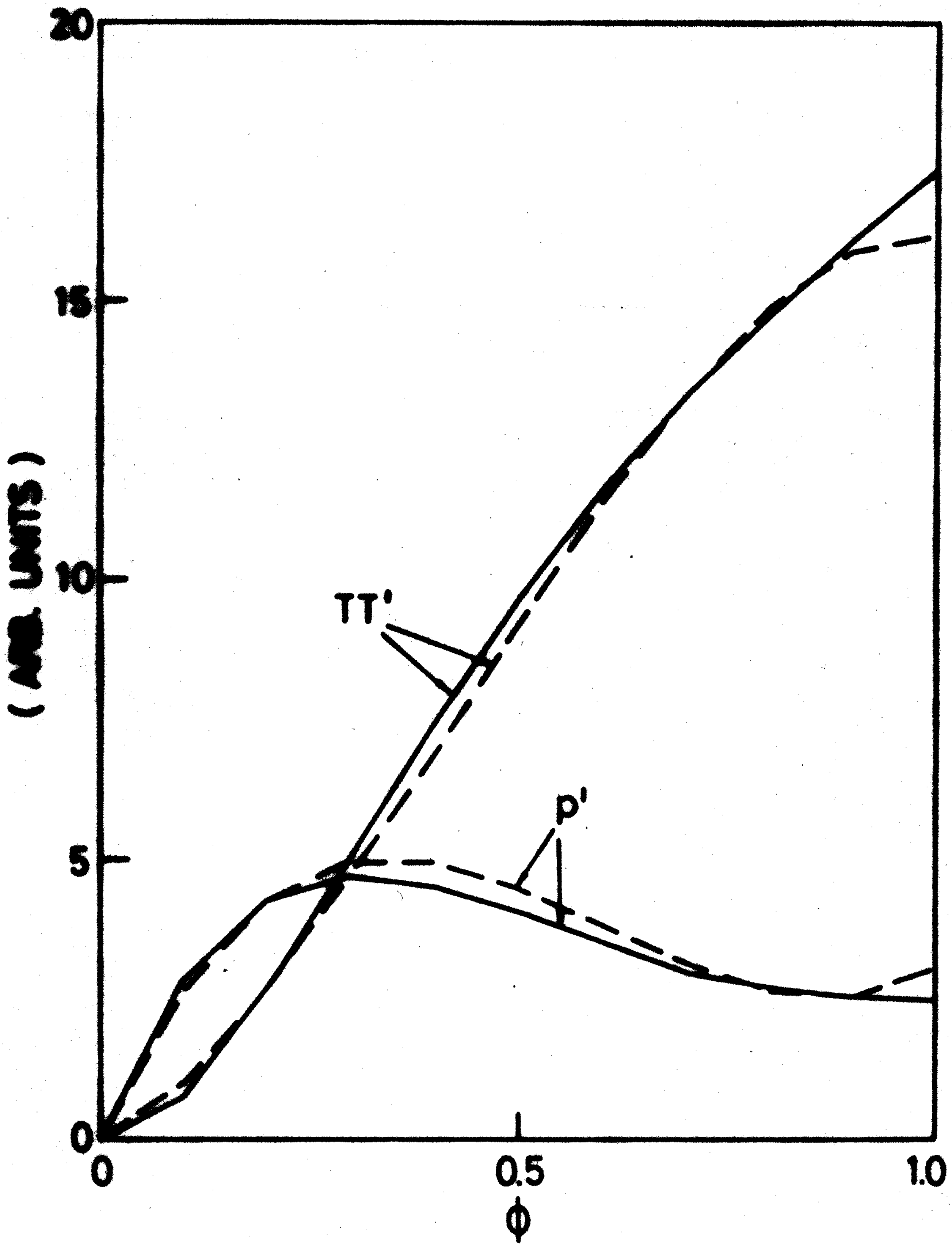

FIG. 4

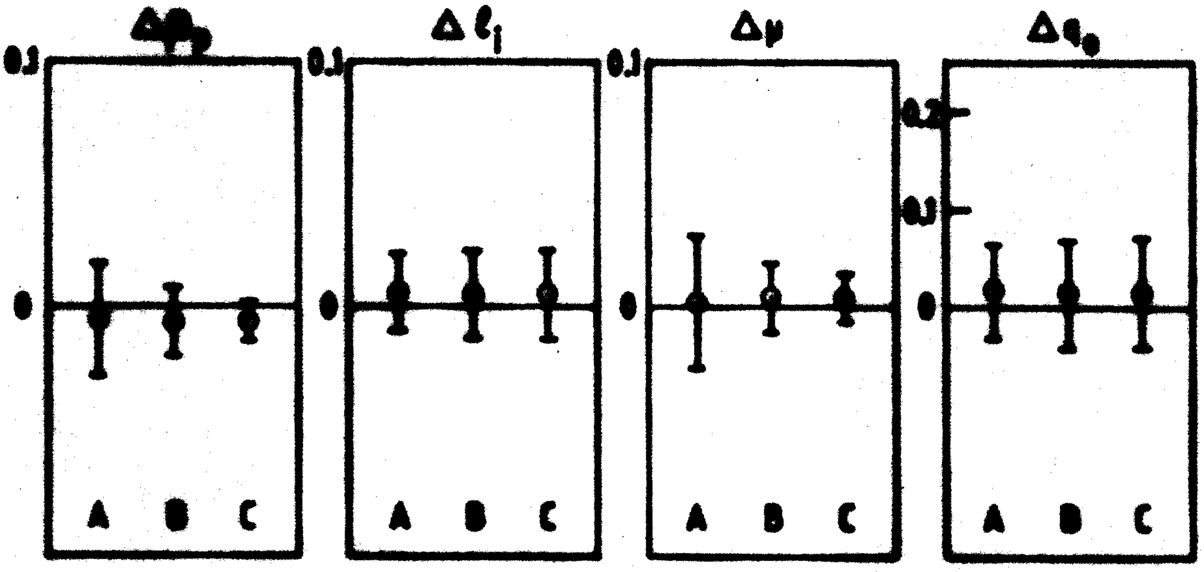

FIG. 5

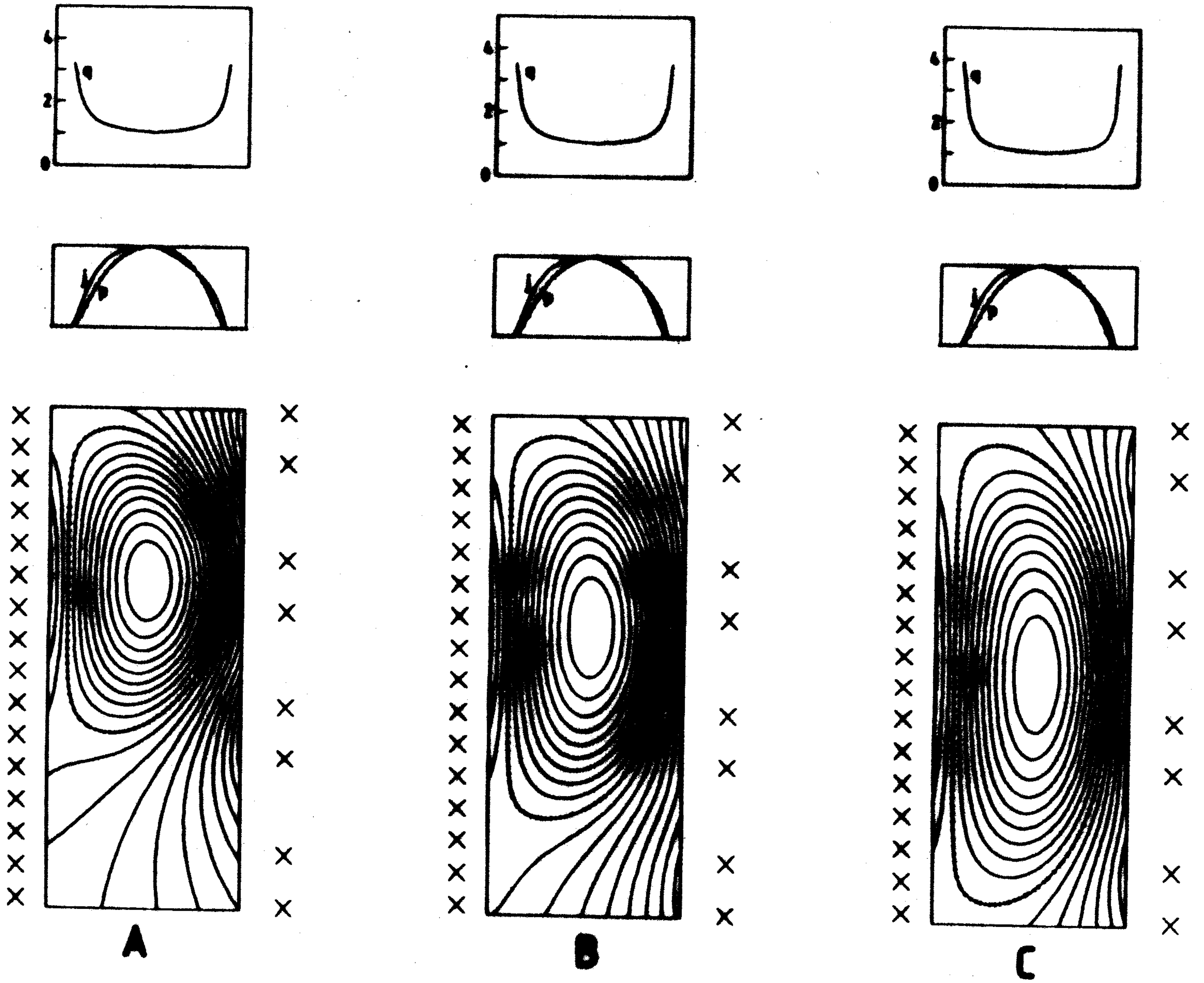

FIG.6

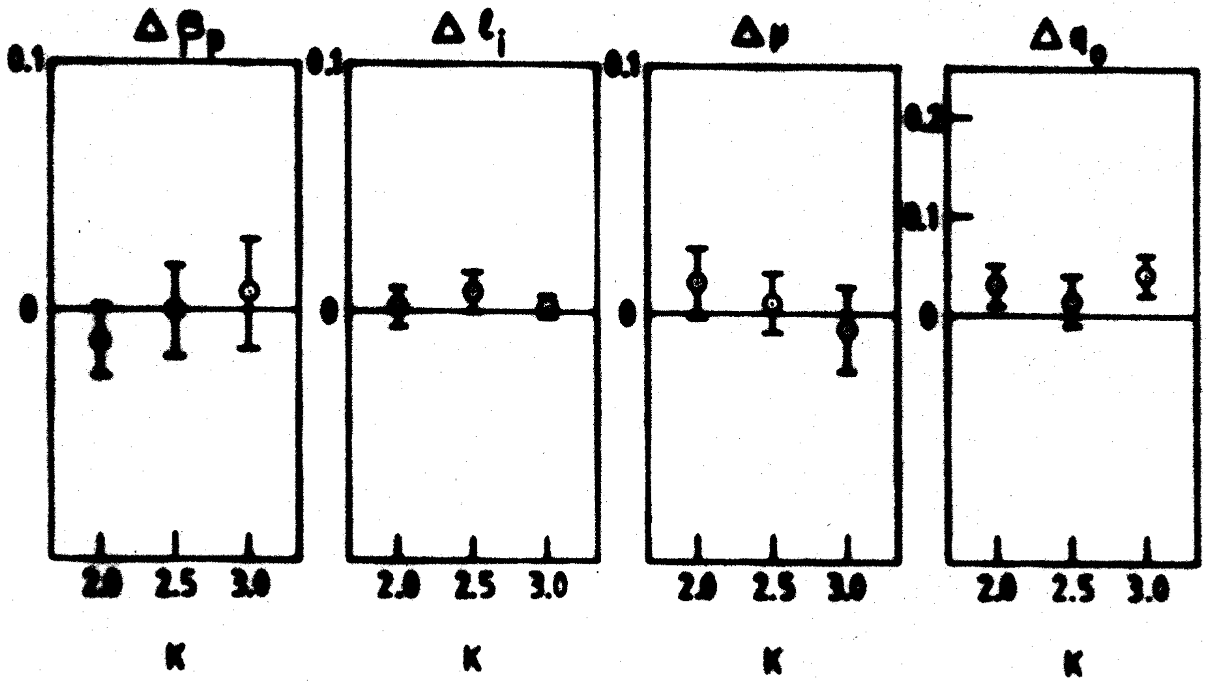

FIG.7